



HAL
open science

**Sorption of Cm(III) and Eu(III) onto clay minerals
under saline conditions: Batch adsorption,
laser-fluorescence spectroscopy and modeling**

Andreas Schnurr, Remi Marsac, Thomas Rabung, Johannes Lützenkirchen,
Horst Geckeis

► **To cite this version:**

Andreas Schnurr, Remi Marsac, Thomas Rabung, Johannes Lützenkirchen, Horst Geckeis. Sorption of Cm(III) and Eu(III) onto clay minerals under saline conditions: Batch adsorption, laser-fluorescence spectroscopy and modeling. *Geochimica et Cosmochimica Acta*, 2015, 151, pp.192 - 202. 10.1016/j.gca.2014.11.011 . hal-01904333

HAL Id: hal-01904333

<https://hal.science/hal-01904333>

Submitted on 24 Oct 2018

HAL is a multi-disciplinary open access archive for the deposit and dissemination of scientific research documents, whether they are published or not. The documents may come from teaching and research institutions in France or abroad, or from public or private research centers.

L'archive ouverte pluridisciplinaire **HAL**, est destinée au dépôt et à la diffusion de documents scientifiques de niveau recherche, publiés ou non, émanant des établissements d'enseignement et de recherche français ou étrangers, des laboratoires publics ou privés.

Accepted Manuscript

Sorption of Cm(III) and Eu(III) onto clay minerals under saline conditions:
Batch adsorption, Laser-fluorescence spectroscopy and modeling

Andreas Schnurr, Rémi Marsac, Thomas Rabung, Johannes Lützenkirchen,
Horst Geckeis

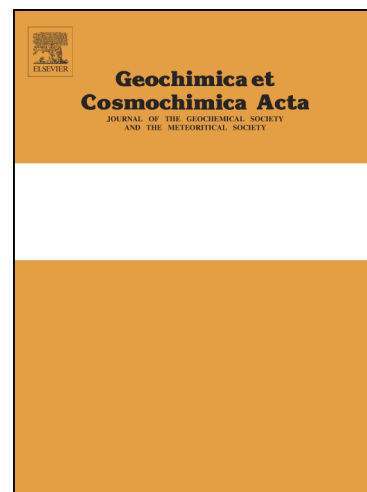
PII: S0016-7037(14)00681-4
DOI: <http://dx.doi.org/10.1016/j.gca.2014.11.011>
Reference: GCA 9050

To appear in: *Geochimica et Cosmochimica Acta*

Received Date: 30 August 2014
Accepted Date: 15 November 2014

Please cite this article as: Schnurr, A., Marsac, R., Rabung, T., Lützenkirchen, J., Geckeis, H., Sorption of Cm(III) and Eu(III) onto clay minerals under saline conditions: Batch adsorption, Laser-fluorescence spectroscopy and modeling, *Geochimica et Cosmochimica Acta* (2014), doi: <http://dx.doi.org/10.1016/j.gca.2014.11.011>

This is a PDF file of an unedited manuscript that has been accepted for publication. As a service to our customers we are providing this early version of the manuscript. The manuscript will undergo copyediting, typesetting, and review of the resulting proof before it is published in its final form. Please note that during the production process errors may be discovered which could affect the content, and all legal disclaimers that apply to the journal pertain.



**Sorption of Cm(III) and Eu(III) onto clay minerals
under saline conditions: Batch adsorption, Laser-
fluorescence spectroscopy and modeling**

Andreas Schnurr^{*}, Rémi Marsac, Thomas Rabung, Johannes Lützenkirchen, Horst Geckeis

Institute of Nuclear Waste Disposal, Karlsruhe Institute of Technology, 76344

Eggenstein-Leopoldshafen, Germany

* Corresponding author: Tel +49 721 608 24325

E-mail address: andreas.schnurr@kit.edu

Abstract- The present work reports experimental data for trivalent metal cation (Cm/Eu) sorption onto illite (Illite du Puy) and montmorillonite (Na-SWy-2) in NaCl solutions up to 4.37 molal (m) in the absence of carbonate. Batch sorption experiments were carried out for a given ionic strength at fixed metal concentration ($[\text{Eu}]_{\text{total}} = 2 \times 10^{-7}$ mol/kg, labeled with ^{152}Eu for γ -counting) and at a constant solid to liquid ratio (S:L = 2 g/L) for $3 < \text{pH}_m < 12$ ($\text{pH}_m = -\log m_{\text{H}^+}$). The amount of clay sorbed Eu approaches almost 100% (with $\log K_D > 5$) for $\text{pH}_m > 8$, irrespective of the NaCl concentration. Variations in Eu(III) uptake are minor at elevated NaCl concentrations. Time-resolved laser fluorescence spectroscopy (TRLFS) studies on Cm(III) sorption covering a wide range of NaCl concentrations reveal nearly identical fluorescence emission spectra after peak deconvolution, i.e. no significant variation of Cm(III) surface speciation with salinity. Beyond the three surface complexes already found in previous studies an additional inner-sphere surface species with a fluorescence peak maximum at higher wavelength ($\lambda \sim 610$ nm) could be resolved. This new surface species appears in the high pH range and is assumed to correspond to a clay/curium/silicate complex as already postulated in the literature for kaolinite. The 2 site protolysis non-electrostatic surface complexation and cation exchange sorption model (2SPNE SC/CE) was applied to describe Eu sorption data by involving the Pitzer and SIT (specific ion interaction) formalism in the calculation of the activities of dissolved aqueous species. Good agreement of model and experiment is achieved for sorption data at $\text{pH}_m < 6$ without the need of adjusting surface complexation constants. For $\text{pH}_m > 6$ in case of illite and $\text{pH}_m > 8$ in case of montmorillonite calculated sorption data systematically fall below experimental data with increasing ionic strength. Under those conditions sorption is almost quantitative and deviations must be

discussed considering uncertainties of measured europium concentrations in the range of analytical detection limits.

Keywords: actinides, lanthanides, trivalent, sorption, saline, TRLFS, modeling, 2SPNE SC/CE, Pitzer, SIT, illite, montmorillonite, clay.

ACCEPTED MANUSCRIPT

1. INTRODUCTION

The final disposal in deep geologic formations is considered the most appropriate strategy to isolate high level nuclear waste (HLW) from the biosphere (e.g. OECD/NEA, 2008). A multi-barrier-system consisting of technical, geotechnical and geological barriers aims at minimizing or even preventing water access to the waste form and the potential radionuclide release from the repository near field. Due to the high sorption capability and capacity of clay minerals, their swelling properties and their low water permeability, these solids are considered suitable materials for geotechnical and geological barriers. Therefore, several countries have selected clay formations as host rock for deep geological disposal: Opalinus Clay, Switzerland (Nagra, 2002); Boom and Ypresian clays, Belgium (Ondraf, 2001); Callovo-Oxfordian and Toarcian clays, France (Bonin, 1998; Andra, 2001). Illite, montmorillonite and illite/montmorillonite mixed layers are the most important components of the proposed claystone host rocks and often amount up to 50 or more wt. % of the material (Bradbury and Baeyens, 2009). Previous sorption investigations (Gorgeon, 1994; Bradbury and Baeyens, 1997, 2002, 2009; Bradbury et al., 2005) were typically carried out at “lower” ionic strength ($I = 0.1$ mol/kg) with only a few single sorption investigations up to 1.0 molal. Clay rock pore waters as e.g. in the Jurassic and lower Cretaceous clay rock in Northern Germany, which are also discussed as potentially appropriate host rock formations, may contain salt contents as high as about 4.9 molal (Brewitz, 1980). Sedimentary rocks currently investigated in Canada are in contact with brine solutions up to 6.5 molal (Fritz and Frape, 1982). At such high salt concentrations, activity coefficients of aqueous species change dramatically. Furthermore, ionic strength effects may significantly affect uptake of strongly

sorbing radionuclides. Detailed sorption investigations are thus necessary to understand radionuclide sorption to clay minerals under saline conditions.

Investigations at high ionic strength need to consider suitable approaches to calculate accurate solution activity coefficients and the applicability of existing surface complexation models has to be assessed for such conditions. Formation of additional surface species that include background electrolyte ions has to be examined. Only few studies deal with radionuclide sorption onto clay materials under saline conditions as recently reviewed by Vilks (2011). A surface complexation approach is described by Ams et al. (2013) while studying the adsorption of Np onto bacteria at high ionic strength. They observed enhanced Np adsorption at increasing the NaClO₄ background concentration from 2.2 m to 4.9 m and modeled their data using a non-electrostatic surface complexation model deriving conditional constants (i.e. constants on the concentration scale without extrapolation to infinite dilution), which restricts the general applicability of this approach.

To the best of our knowledge no systematic sorption study is presently available dealing with nearly saturated salt solutions, where radionuclide uptake, spectroscopic and modeling studies are combined.

Illite and montmorillonite are layered alumino-silicates with a repetition of TOT (tetrahedron-octahedron-tetrahedron) layers. Isomorphous substitutions within the lattice cause a permanent negative charge. In illite, with a higher substitution degree than montmorillonite, negative charge is mainly compensated by potassium cations located in the interlayers. This fact is responsible for the absence of swelling properties and the lower cation exchange capacity as compared to montmorillonite. Both types of clay are characterized by permanently

negatively charged basal planes and amphoteric hydroxyl groups at the edge planes. As a consequence trivalent lanthanide/actinide cations predominately bind to basal planes in an outer-sphere mode via cation exchange reactions at low pH and low ionic strength. With increasing pH inner-sphere complexation at the edges occurs as has been verified by spectroscopic methods (Stumpf et al., 2001, 2002; Geckeis and Rabung, 2008; Tan et al., 2010; Geckeis et al., 2013).

A frequently applied model to describe the interactions of various radionuclides with clay minerals has been developed by Bradbury and Baeyens (1997, 2002). This quasi mechanistic 2 site protolysis non-electrostatic surface complexation and cation exchange (2SPNE SC/CE) model was used to successfully describe titration, sorption edge and sorption isotherm data over a wide pH range (3 - 12) up to background electrolyte concentrations of about 1 molal (NaClO_4).

The major objective of the present paper is to test the applicability of the 2SPNE SC/CE model to highly saline conditions. We present experimental sorption/uptake data that are required for this test and supply speciation insight by the application of *in-situ* time-resolved laser fluorescence spectroscopy (TRLFS) studies.

2. MATERIALS AND METHODS

2.1. Clay materials

Clay materials were obtained as aqueous suspensions from the Laboratory for Waste Management (LES) of the Paul Scherrer Institute (PSI), Switzerland. The preparation and pretreatment (Bradbury and Baeyens, 2009) of the Illite du Puy and Na-SWy-2 montmorillonite along with details of the experimental methodologies have been described in

much detail in a number of previous publications (Poinssot et al., 1999; Bradbury and Baeyens, 2002, 2009; Baeyens and Bradbury, 2004). Relevant information such as N₂-BET surface area and cation exchange capacity is available in these references and will not be repeated here. All suspensions were stored in the dark at 4 °C prior to use and utilized within one year after preparation.

2.2. Chemicals

NaCl, to fix background electrolyte concentrations, NaOH and HCl for pH adjustment, were obtained from Merck (pro analysi) and used without further treatment.

Eu(III) was used for batch sorption experiments as a homologue for trivalent actinides. Eu solutions were prepared from ICP Standard Merck stock solutions 6.58×10^{-3} mol/kg (5% HNO₃) and spiked with a radiotracer solution (total Eu concentration: 6.0×10^{-4} mol/kg; isotopic composition: ¹⁵¹Eu(83%), ¹⁵²Eu(13%, $t_{1/2} = 13.33$ a), ¹⁵³Eu(4%)). ¹⁵²Eu is a β-, γ-emitter and can conveniently be used in γcounting for precise determination of dissolved ¹⁵²Eu. The Eu radiotracer solution was purchased from Amersham International. For TRIFS studies Cm was used as a fluorescence probe. The isotopic composition of the Cm solution is 89.68% ²⁴⁸Cm, 9.38% ²⁴⁶Cm, 0.43% ²⁴³Cm, 0.30% ²⁴⁴Cm, 0.14% ²⁴⁵Cm and 0.07% ²⁴⁷Cm.

2.3. Experimental procedures

All experiments were carried out under controlled argon atmosphere in glove boxes (O₂ ~ 2 ppm) at room temperature (~ 25 °C). Eu sorption measurements were carried out as a function of pH at constant ionic strength and solid to liquid ratio. In the present study, measurements of operational pH values were made on an Orion 2 Star Benchtop pH meter using an Orion

8103SC combination pH electrode. Commercial pH Titrisol buffer solutions (Merck p.a.) were used to calibrate the setup.

For pH measurements in highly saline conditions ($I > 0.1$ mol/kg) a correction term is applied for the measured operational pH-values (pH_{exp}). In the present case the molal proton concentration, i.e. $-\log m_{H^+}$ (pH_m), was obtained in the following way. An empirical correction coefficient (A) that depends on background electrolyte composition and concentration and that has been accurately determined for NaCl solutions by Altmaier et al. (2003), was used to derive the operational pH_{exp} values according to equations 1 and 2

$$pH_m = pH_{exp} + A_{NaCl} \quad (1)$$

$$A_{NaCl} = 0.0013 * (m_{NaCl})^2 + 0.1715 * m_{NaCl} - 0.0988 \quad (2)$$

where m_{NaCl} is the molality (mol/kg) of the background electrolyte.

Different target pH_m -values were achieved in our experiments by addition of NaOH and HCl. No pH buffer solutions were used (except for some selected experiments, where this will be explicitly mentioned). The equilibration time for the uptake experiments was at least 96 hours. Batch sorption investigations were carried out for three different salt concentrations ($m_{NaCl} = 0.10, 0.92, 3.90$ mol/kg) at fixed Eu concentration ($m_{Eu, total} = 2 \times 10^{-7}$ mol/kg) and fixed solid to liquid ratio (2 g/L) for both clays under exclusion of CO_2 . Separate samples were prepared with different pH_m values (pH range: 3 - 12; step width ~ 0.5) in HDPE (high-density polyethylene) vials (Zinsser). For phase separation, the suspensions were transferred to special centrifuge tubes (Beckmann, Recorder No.: 356562) and centrifuged (Beckmann Coulter XL-90K) at 90000 rpm (~ 700000 g max) for one hour. After complete phase

separation, radionuclide analysis was performed in the liquid phase using a Perkin Elmer Wallac gamma counter (Wizard 1480) with a subsample of the supernatant.

Sorption data are presented as percentage adsorbed and as the logarithm of the distribution ratio (K_D) for a better comparison to previously published data. The K_D -value is defined as

$$K_D = \frac{m_{init.} - m_{eq.}}{m_{eq.}} * \frac{V}{m} \quad (3)$$

where m_{init} is the total initial sorbate concentration (mol/kg), m_{eq} the aqueous sorbate concentration at equilibrium (mol/kg), V the volume of liquid phase (L) and m the mass of solid phase (kg).

For the TRFLS measurements a pulsed Nd:YAG dye laser system (Continuum Surelite II, Radiant dyes Narrow Scan, repetition rate: 10 s^{-1}) was operated at a constant excitation wavelength of 396.6 nm with the dye Exalite 398. Fluorescence emission at a laser energy of 2 - 3 mJ was detected by an optical multichannel analyzer consisting of a polychromator (Shamrock 303i, Andor) with a 1200 lines/mm grating resulting in an active wavelength range of 580 - 620 nm and a ICCD-camera (iStar, Andor; camera controller on PCI-card). Spectra were measured 1 μs after the laser pulse in a time window of 1 ms. Fluorescence lifetime measurements were performed by monitoring the fluorescence emission as a function of the delay time between the laser pulse and the camera gating. Delay time steps were kept constant at 10 μs .

The experimental procedure in the TRFLS work was similar to the batch sorption investigations. The solid to liquid ratio was lowered by one order of magnitude in the TRFLS

experiments (S:L = 0.25 g/L) to reduce the strong effect of light absorption/scattering of the incident laser beam as well as of the fluorescent emission light. The TRLFS spectra of Cm in the presence of clay minerals were studied in NaCl background electrolyte concentrations of 0.10, 1.02 and 4.37 mol/kg. The initial Cm concentration was $m_{\text{Cm}} = 2 \times 10^{-7}$ mol/kg. To study the potential influence of dissolved silica on Cm speciation different Si concentrations ($m_{\text{Si}} = 10^{-5}$, 10^{-4} and 10^{-3} mol/kg) were equilibrated with $m_{\text{Cm}} = 2 \times 10^{-7}$ mol/kg in the presence of illite. To keep $\text{pH}_m = 9$ TRIS buffer solution (Merck, p.a.) was used.

2.4. Calculations

We used the computer program PHREEQC (Parkhurst and Appelo, 1999), which has a built-in ability to handle both Pitzer equations and adsorption modeling, to simulate the systems even at high ionic strength. As we applied a non-electrostatic sorption model, there was no need to select a specific surface charge model to simulate surface complex reactions. The Gaines and Thomas formalism (1953) was used to calculate sorption for the Eu^{3+} - Na^+ exchange on the planar sites of the clay minerals. The activity corrections, the Harvie-Moller-Weare HMW Pitzer data base (Harvie et al., 1984) and the Pitzer coefficients for the Cm/Eu species from Neck et al. (2009), were implemented in PHREEQC. This program also has a built-in SIT option. The SIT formalism is less complex than the Pitzer formalism, but restricted to $I < 3 - 4$ mol/kg. SIT coefficients for the Cm/Eu species were taken from Neck et al. (2009).

We verified that the calculations involving the Pitzer formalism and an adsorption model gave consistent results. To this end a code comparison was carried out. One set of model calculations was performed using the program ECOSAT 4.8 (Equilibrium Calculation of

Speciation and Transport, Keizer and van Riemsdijk, 1999). This code does not include the Pitzer formalism and activity corrections must be done separately. The activity coefficients were obtained by the code The Geochemist's Workbench (GWB; Bethke and Yeakel, 2011) with the same Pitzer parameter set as that was used for calculations with PHREEQC. In ECOSAT the conditional constants were inserted and activity corrections were switched off, so that all calculations could be done on the concentration scale. The cross check was deemed useful since we are not aware of any previously published surface complexation modeling that involves the Pitzer formalism. Applying the Pitzer formalism requires many parameters in the respective data bases of GWB and PHREEQC and cases have been documented where different speciation codes give different results although identical parameter sets have been used (e.g. Gustafsson and Lumsdon, 2014). Use of ECOSAT requires several steps including separate calculation of species activity coefficients, water activity and calculation of conditional stability constants. Details are given in Supplementary Information. There are no fundamental differences between the two ways of calculations.

Eu sorption onto illite and montmorillonite is modeled with the 2 site protolysis non-electrostatic surface complexation and cation exchange (2SPNE SC/CE) sorption model (Bradbury and Baeyens, 1997, 2002). The model considers two types of high surface density protolysable (W1 and W2) sites to simulate clay proton titration data. In the latest version of the model (Bradbury and Baeyens, 2009), only strong sites, S, have been considered for modeling cation surface complexation data at trace metal ion concentrations. All model parameters (i.e. aqueous species, surface hydroxyl group density, cation exchange capacity, surface species and thermodynamic constants) are taken from NEA (2003) and Bradbury and

Baeyens (2006, 2009). The constants are presented in tables 1, 2 and 3 all extrapolated to zero ionic strength conditions. No separate activity corrections are involved for the surface species, i.e. in the mass law equations only activity coefficients for dissolved species and activity of water have to be considered to calculate the ionic strength dependence of stability constants. Two assumptions are made for the predictive modeling at higher ionic strength: a) the established Eu surface species remain unaffected by changes in ionic strength and b) all surface sites remain available even at high NaCl concentration, where coagulation of clay particles might cause blocking of surface sites.

3. RESULTS AND DISCUSSION

3.1. Sorption onto illite (Illite du Puy)

The uptake of Eu onto illite is presented as percentage sorbed (Fig. 1a) and $\log K_D$ (Fig. 1b, c and d) versus pH_m . The sorption edges include replicate measurements from two years apart (2010 and 2012) with two different clay batches. The data points obtained with the two batches are plotted together in figure 1. They do not differ significantly.

The general pH_m dependent sorption of trivalent metal cations onto clay minerals shows the usual features. At low pH_m values and $I = 0.09$ molal, Eu uptake is higher than 50% and reaches nearly 100% for $\text{pH} > 5 - 6$ (Fig. 1a). The uptake in the low pH region is reduced with increasing salt content. The amount of adsorbed Eu at $\text{pH}_m = 3 - 4$ decreases from 50 - 70% for the lowest NaCl concentration (0.09 molal) to nearly no sorption for higher NaCl concentrations (0.92 and 3.90 molal). Also, a slight shift of the sorption edge to higher pH_m with increasing NaCl concentration is observed. Nevertheless, almost complete uptake of Eu ($\geq 99.5\%$) is observed for all investigated NaCl concentrations at $\text{pH}_m \geq 6.5$. The results for

Eu sorption onto illite clearly show that for pH values relevant to nuclear waste disposal ($\text{pH}_m \sim 8$ for typical clay porewater conditions and $\text{pH}_m > 10$ in the presence of cementitious material), at least in pure NaCl solutions and in the absence of carbonate, no significant ionic strength effect is observed. Such a relationship might, however, simply be invisible due to large analytical uncertainties in this pH range. The shaded area in figure 1b represents the region of very high $\log K_D$ values > 6.2 corresponding to $> 99.97\%$ sorption which corresponds to the calculated detection limit of our analytical method (based on the 3σ standard deviation of the background criterion).

Previous studies have shown that cation exchange reactions are the dominant process controlling the uptake of Eu onto illite for $\text{pH}_m < 5$ whereas the surface complexation of Eu to $-\text{OH}$ groups at the edges of illite particles is the dominant process for $\text{pH}_m > 5$. It is well known that cation exchange is suppressed by higher background electrolyte concentrations. It explains the lower Eu uptake for $\text{pH}_m < 5$ and high ionic strengths.

For $6.5 < \text{pH}_m < 9$, sorption data at any ionic strength are not significantly different. Our data are not only in agreement with previous studies (Bradbury and Baeyens, 2009) (performed at low ionic strength) but show also, for the first time, that Eu sorption to illite is not severely affected by highly saline conditions at $\text{pH}_m > 6.5$.

To proof the analogy between Eu(III) and Cm(III) and to show that these two trivalent metals show the same sorption behaviour, we tried to achieve some Cm-illite sorption data from the TRLFS emission spectra in addition to the Eu-illite batch sorption data. These data, shown in figure 1c, were determined by quantifying the amount of aqueous Cm species and calculating the respective $\log K_D$ values. For quantitative spectra evaluation we followed the approach described by Rabung et al. (2005). Considering that TRLFS is not able to distinguish between

Cm aquo species and outer-sphere complexation of these aquo species (as in both cases no change in the first hydration sphere occurs) we could explain the differences for $I = 0.09$ mol/kg. At this ionic strength outer-sphere complexation via cation exchange as well as inner-sphere sorption occurs whereas TRLFS data evaluation only considers the inner-sphere contribution to the overall sorption. For the sorption data in 0.9 molal NaCl, where cation exchange is suppressed we could completely reproduce our Eu batch sorption studies.

The lines in figure 1a represent blind predictions using the 2SPNE SC/CE model calibrated at low ionic strength (0.1 mol/kg NaClO₄ solutions) by Bradbury and Baeyens (2009). Hydrolysis and surface complexation constants at infinite dilution as well as illite surface site density and protolysis constants (tables 1, 2 and 3) were taken from the literature (NEA, 2003; Bradbury and Baeyens, 2006 and 2009) and corrected for each ionic strength using the Pitzer formalism (for $m_{\text{NaCl}} = 0.92, 3.90$ mol/kg) or using the Davies correction (for $m_{\text{NaCl}} = 0.09$ mol/kg). For the surface complexation constants only activity coefficients for the aqueous species and water activity were included (i.e. no activity coefficients for the surface species are involved as in the original model). Blind predictions fit remarkably well the experimental data for $m_{\text{NaCl}} = 0.09$ to 3.90 mol/kg. The calculated Eu surface species distribution for $m_{\text{NaCl}} = 3.90$ mol/kg is also presented in figure 1a to illustrate the simulated sorption edge.

We would like to note here, that the nature and number of surface species required to describing sorption data strongly depend on the applied sorption model. Generally, non-electrostatic models will require more surface species than models including an electrostatic correction term. Also the electrostatic factors include pH-dependence (Stumpf et al. 2008), so that they help outcompete hydrolysis reactions in solution. Insofar, calculated surface

speciation is to some extent speculative. Earlier spectroscopic studies, however, corroborate the existence of the three main surface species SsOEu^{2+} , $\text{SsOEu}(\text{OH})^+$ and $\text{SsOEu}(\text{OH})_2$ and thus support the assumptions underlying the 2SPNE SC/CE model (Stumpf et al. 2001, 2002; Rabung et al., 2005).

Figure 1b and 1c ($\log K_D$) highlights differences between model and experiment that are hidden in the percentage uptake presentation. Indeed, at $\text{pH}_m > 7$ and 0.09 m NaCl a deviation exists between our experimental dataset and the model and, therefore, also with the underlying experimental data of Bradbury and Baeyens (2009). Our $\log K_D$ values are higher and the difference is at about 0.5 $\log K_D$ units, corresponding to 99.97% vs. 99.90% Eu sorbed. Bradbury and Baeyens give an uncertainty of ± 0.5 for their $\log K_D$ (Bradbury and Marques Fernandes, 2013) values in this pH range, where concentrations of dissolved Eu(III) lie close to the detection limit. The simulation shown in figure 1d uses a slight variation of surface complexation constants compared to those given by Bradbury and Baeyens (constants in brackets in Tab. 3) and, therefore, provides an estimate for the uncertainty range of both model prediction and experimental data. Based on such considerations, experimental and modeling data obtained in the present work do not significantly differ from literature data.

We nevertheless explored, whether Eu(III) uptake onto container walls (HDPE analytic vials) or other surfaces (pipette tips, pH electrode etc.) could explain the slightly enhanced Eu(III) sorption in comparison to literature data. While such effects become dominant in blank experiments (i.e. in the absence of clay) at higher pH, they were not observed when clay is present. Dedicated experiments demonstrated clearly (see supplementary information for

details) that in this pH range 99.96 % of the Eu(III) are sorbed to clay minerals solely (Fig. 1b, green stars). Respective $\log K_D$ values are equal to 6.12 - 6.17. A possible origin for slightly varying experimental data in our study as compared to the work of Bradbury and Baeyens might lie in the procedure and/or efficiency of phase separation (e.g. different centrifugation velocities). Quantitative elimination of colloidal clay particles from the suspension still represents a challenge.

While the ionic strength dependent sorption edge is quite well predicted by the model (e.g. Fig. 1a), results predict a reduced sorption with increasing ionic strength at $\text{pH}_m > 6$ (plateau region) This result is independent of the approach to account for activity correction either taking Pitzer (Fig. 1b) or SIT (Fig. 1c). The latter trend is not observed in experimental data or might be simply hidden by analytical uncertainties as has been discussed before (Fig. 1d). The non-observed ionic strength dependence in our experimental data might, however, also have other reasons. One is that ion-ion interactions at the mineral surface at elevated ionic strength may not be any more negligible which would not be accurately described in a purely non-electrostatic model approach. An electrostatic model might predict stronger uptake for all ionic strengths with increasing pH. For example, Stumpf et al. (2008) estimated that the formation constant for an inner-sphere surface complex would increase by one order of magnitude for each positive charge unit that is transferred to a negative surface. Since this is compatible with our system (i.e. the cation is adsorbed to a net negatively charged clay particle), such an additional ionic strength effect could overcompensate aqueous speciation effects.

In addition surface speciation and sorption extent of Eu(III) can be influenced at increased Cl⁻ concentration by formation of ternary chloride complexes. Such ternary Eu surface complexes would contribute to the uptake and this would be enhanced with increasing chloride concentration. This possibility can to some extent be tested by spectroscopy (TRLFS) provided that inner-sphere chloro complexes form at the surface (see discussion below). Overall, the underprediction for $6.5 < \text{pH}_m < 9$ never exceeds one log K_D unit (Fig. 1b, c) and is not even visible in the percentage uptake curves. In all, the present blind modeling results may therefore be considered as quite promising.

Calculations performed with SIT are presented (Fig. 1c) to compare the application of the two formalisms for activity corrections at high salt content. Both formalisms show consistent results. The decrease of log K_D with increased ionic strength for $\text{pH}_m > 7$ is slightly less pronounced for the SIT option. For the purpose of the work described here, SIT thus appears to be a quite appropriate method to account for ionic strength effects in solution. SIT has the advantage that respective parameters for a significant number of nuclear waste disposal relevant ionic species are abundant from the OECD/NEA databases. We furthermore did not observe any significant differences in calculated results taking either PHREEQC or ECOSAT in combination with The Geochemist's Workbench.

Various aspects of the observed difference of calculated and experimental data can be discussed:

- Due to the very low Eu(III) concentrations at analytical detection limits found in solutions at $\text{pH}_m > 9$, the actual K_D values could be even higher than assumed in this

work. Small differences in measured concentrations due to slight variations in the efficiency of colloid separation by centrifugation thus can make a strong effect.

- Since our experimental distribution coefficients for $pH_m > 9$ exceed the detection limit, it is not possible to conclude whether the predicted trend in sorption with increasing ionic strength also occurs in the experimental data.

3.2. Sorption onto montmorillonite (Na-SWy 2)

As for illite, two separate sets of experimental data (collected in 2010 and 2012 for each ionic medium, respectively) are plotted in figure 2 as $\log K$ (percentage uptake is shown in supplementary information figure 6SI) versus pH_m . This shows that the reproducibility is excellent. The general trend found for the influence of pH_m and ionic strength on Eu uptake that was observed for illite is also retrieved for the montmorillonite: (i) Eu uptake increases with pH_m , (ii) an increase in ionic strength suppresses the contribution of cation exchange (i.e. for $pH_m < 6$) and (iii) for $pH_m > 9$ Eu uptake cannot be accurately quantified (i.e. distribution coefficients are at and above the detection limit). Because of the latter point, a potential ionic strength dependence that is suggested by the model cannot be experimentally verified. Again, it is evident that the scattering of data points for $\log K_D > 5$ lie in a range of at least ± 0.5 log units, consistent with observations reported above and in the literature for this pH range. For the montmorillonite, the shift in the pH edge with increasing ionic strength is more pronounced. Indeed, the ionic strength clearly affects Eu uptake onto montmorillonite up to $pH_m = 8 - 9$ whereas in case of illite experimental data are more or less independent of ionic strength at $pH_m > 6.5$. For $pH_m > 6$ and all ionic strengths, Eu uptake on the montmorillonite is pH-dependent and in this region surface complexation is the dominant sorption mechanism.

Therefore, the ionic strength effect on Eu(III) sorption for $6 < \text{pH}_m < 8 - 9$ is unlikely to be due to a cation exchange competition by Na^+ .

The lines in figure 2 show the blind predictions based on the model (Bradbury and Baeyens, 2006) using stability constants at infinite dilution given in tables 1, 2 and 3. Ionic strength corrections were carried out using the Pitzer equations (Fig. 2). Application of the SIT approach (shown in the supplementary information figure 7SI) leads to the same conclusions as for illite.

For $m_{\text{NaCl}} = 0.09 \text{ mol/kg}$, the blind predictions are in very good agreement with the experimental data of this study and, consequently also with the underlying experimental data of Bradbury and Baeyens (2006) up to $\text{pH}_m = 10$.

However, there are some details that need to be addressed:

The dip in the calculated distribution coefficient at $\text{pH}_m > 11$ (which was not observed in figure 1b, c) could be explained by the fact that Bradbury and Baeyens (2006) studied Am/Eu uptake to montmorillonite only for $\text{pH}_m < 10$. The complexation constant for the $\equiv\text{S}^{\text{O}}\text{Eu}(\text{OH})_3^-$ species that was used for describing illite sorption data and which is relevant for $\text{pH}_m > 11$ (Fig. 1a) is not available for montmorillonite. For a better and consistent fit of the experimental data we introduced such a species in the present study with a log K value of -25.8 (Tab. 3 value in brackets) which is within the range of the LFER approach (Bradbury and Baeyens, 2006) to -27.8 ± 2 . There is still a small dip at high $\text{pH}_m > 11$. A further increase of this constant would significantly improve the fit but then the value would be outside the range of the LFER approach.

For the high salt contents, cation exchange is quite well predicted (i.e. for $\text{pH}_m < 6$). A decrease in $\log K_D$ is observed with increasing ionic strength in the pH range where surface complexation prevails (as has been discussed for illite). This can only be seen in $\log K_D$ plots (Fig. 2a, b).

Compared to illite, for $\text{pH}_m > 8$, the discrepancies between experimental data and predictions are slightly smaller. For $6 < \text{pH}_m < 8$, Eu sorption is almost unaffected by ionic strength for illite and the model under predicts Eu uptake at higher ionic strength. The opposite is observed for montmorillonite. A possible reason for the small deviation of experimental and calculated data in this pH range might be that montmorillonite, which is known to be completely delaminated at low ionic strength, is more prone to salt induced aggregation possibly via edge/plane interaction (e.g. Tombácz et al., 2004) with concomitant reduction of available surface sites. In this study we obtained comparable Eu sorption data for illite and montmorillonite for the lowest ionic strength. With increasing ionic strength the discrepancies between illite and montmorillonite increase (less Eu sorption in the SWy-2 system for high ionic strength). This effect could also be explained by coagulation/aggregation effects which are more pronounced for montmorillonite. This is supported by two further observations reported in the literature:

- (i) Gorgeon (1994) investigated Am sorption onto montmorillonite for $I = 0.1$ and 1.0 mol/kg. Based on this experimental data set, Am(III) surface complexation constants to montmorillonite were determined by Bradbury and Baeyens (2006). $\log K$ for $\equiv\text{S}^{\text{O}}\text{Am}^{2+}$ differs by 0.6 log units when taking data obtained at $I = 0.1$ mol/kg as compared to the data set for 1.0 molal, while the same stability constants

irrespective of ionic strength were assigned to the other surface species. The trend is consistent with the present experimental results, where a decreased uptake is observed for $\text{pH}_m < 7$ (i.e. in the range where $\equiv\text{S}^{\text{S}}\text{OEu}^{2+}$ is the dominant surface species).

- (ii) Ca^{2+} is known to be an even stronger coagulant for montmorillonite than Na^+ . For Ca-montmorillonite Bradbury and Baeyens obtained a log K value for the formation of $\equiv\text{S}^{\text{S}}\text{OEu}^{2+}$ that is more than one order of magnitude lower than for Na-montmorillonite. Again the stability constants for the other surface species remain unchanged (Bradbury and Baeyens, 2006).

Nevertheless, the blind prediction using a unique set of stability constants fits the experimental data within the uncertainties of constants and experimental data fairly well.

A final remark should be made concerning the Pitzer data set (Neck et al., 2009) used in this study. The data set was mainly evaluated from solubility experiments in CaCl_2 . During the modeling it was found out that some ternary parameters in the NaCl system were set to zero due to a lack of experimental data (see supplementary information). As a consequence the chloride complexes of the trivalent ions decrease with increasing chloride concentrations. The effect is small and does not affect surface complexation calculations significantly, which is also demonstrated by the fact that SIT virtually provides identical results.

3.3. TRLFS studies

One model inherent assumption is that the stoichiometry of the Cm/Eu surface species is not affected by the huge variation in NaCl concentration, while it cannot be excluded a priori that Cm/Eu surface complexes involving co-adsorption of chloride contribute to the overall uptake

at high chloride concentrations. Aqueous Cm-chloride complexes have been identified in previous TRLFS studies (Fanghänel et al., 1995), however are considered irrelevant up to concentrated NaCl concentrations. Even though, to test the possibility of ternary chloro surface complex formation, Cm TRLFS studies in the clay-systems were performed.

TRLFS involving Cm is an extremely sensitive spectroscopic method for in-situ speciation. The Cm ${}^6D_{7/2} \rightarrow {}^8S_{7/2}$ transition energy depends on the environment of the first coordination sphere. As a consequence the emission band of the free Cm³⁺_{aqo}-ion ($\lambda = 593.8$ nm) is shifted to higher wavelengths when inner-sphere complexation occurs. The degree of these shifts depends on the nature of the ligands and in general increases with the number of ligands per Cm. The Cm/clay systems show different emission spectra with varying pH (Rabung et al., 2005).

The Cm/Na-illite (Na-SWy-2) system ($m_{\text{Cm}} = 2 \times 10^{-7}$ mol/kg, S:L ratio = 0.25 g/L) was investigated at $m_{\text{NaCl}} = 0.10, 1.02$ and 4.37 mol/kg over a wide pH range. The full set of measured emission spectra is shown in supplementary information exemplarily for $m_{\text{NaCl}} = 0.10$ mol/kg and for selected pH_m -values in figure 3. The emission spectra exhibit a shift with increasing pH_m . The spectra obtained at each pH_m -value typically consist of a mixture of different surface and aqueous species.

Peak deconvolution of the spectra for each ionic strength results in a minimum of single compounds of four inner-sphere surface species. They exhibit emission band peak-maxima for illite (in brackets for montmorillonite) at approximate 598.5 (598.5), 602.5 (602.4), 605.6 (605.8) and 610.2 (610.4) nm (± 0.2 nm) (Fig. 4). In addition, small contributions of aqueous Cm chloride 1:1 and 1:2 complexes were detected at low pH_m for high ionic strength. Because of the difficulties to extract pure component spectra of each inner-sphere sorbed species from

all mixed spectra and as generally more than two different Cm species exist simultaneously, small variations could not be excluded for the single component spectra. This is further complicated due to the well-known decreasing fluorescence intensities with increasing pH_m values, leading to more scattered spectra at higher pH_m . The emission band for the inner-sphere surface complex appearing at low pH is difficult to extract at increasing ionic strength as the abundance of this species is low because of the shift of the sorption edges with ionic strength (Fig. 1, 2). The first three inner-sphere complexes can be assigned to the same surface species that had been previously reported for illite and montmorillonite (Rabung et al., 2005): $>\text{SOCm}(\text{H}_2\text{O})_5^{2+}$, $>\text{SOCm}(\text{OH})(\text{H}_2\text{O})_4^+$, $>\text{SOCm}(\text{OH})_2(\text{H}_2\text{O})_3$ (Tab. 3). Unlike previous studies, an additional inner-sphere surface species with a higher peak shift was observed at high pH_m . The absence of this species in previous work (Rabung et al., 2005) might be explained by the improved quality of the spectra that were obtained by a more efficient detection system in the present work. Also, the pure component spectrum of the “high-pH species” (i.e. the “third” surface species) obtained by Rabung et al. (2005) was quite broad and may cover more than one single species.

From the compilation of all pure component spectra for the different electrolyte solutions (Fig. 4) no significant influence of NaCl background electrolyte concentration on Cm surface speciation exists. Even at $m_{\text{NaCl}} = 4.37$ mol/kg, peak deconvolution results in the four inner-sphere surface species with approximately the same emission band positions. This corroborates our modeling assumptions in having identical surface species independent of NaCl ionic strength.

Fluorescence lifetime (τ) measurements up to weakly alkaline pH conditions show in addition to the $\text{Cm}^{3+}_{\text{aquo}}$ -ion with $\tau = 68 \pm 2$ μs a lifetime component of $\tau \sim 113 \pm 10$ μs ($\sim 120 \pm 15$ μs

for montmorillonite) which can be attributed to inner-sphere surface species in agreement with previous results (Rabung et al., 2005). Calculating the number of H₂O/OH⁻ ligands remaining in the first coordination sphere for the surface sorbed species from these lifetime values in comparison to the nine-fold hydrated Cm³⁺_{aq}-ion, we obtain 4.8 ± 0.3 (4.5 ± 0.6) comparable to previous studies. The lifetime measurements support the results and interpretations based on the fluorescence emission spectra that there is no ionic strength dependency for the different inner-sphere sorption species. Additional inner-sphere coordinated chloride would lead to a further increase of the fluorescence lifetime. In view of the decreasing H₂O activity at high NaCl concentrations, the unchanged number of water molecules in the first Cm(III) coordination sphere is certainly remarkable and points to a strong binding to the central metal ion.

Additional experiments have been performed to resolve the nature of the previously undetected inner-sphere Cm surface complex with a fluorescence wavelength at the peak maximum of about 610 nm. Huittinen et al. (2012) have observed a similar species in their Cm sorption study on kaolinite and assigned this species to a mixed clay/curium/silicate surface complex. Due to enhanced Si (and Al) dissolution of the clay at higher pH ($\text{pH}_m > 10$) the formation of such a mixed surface species was considered possible and validated by subsequent TRLFS experiments, in which Al and/or Si had been added to the system. Following this approach, we added different amounts of Si to a Cm illite suspension at $\text{pH}_m = 9$ (fixed by Merck pH buffer solution). At this pH the 610 nm species was not detected in the Cm-illite spectra and for $\text{pH}_m < 10$ no increased Si concentrations were found due to clay dissolution (Bradbury and Baeyens, 2009).

Figure 5 shows that at lower concentrations of added Si (10^{-5} and 10^{-4} mol/kg), no significant effect is observed compared to the system without Si addition. The peak maximum of the emission spectra could be assigned to the $>\text{SOCm}(\text{OH})(\text{H}_2\text{O})_4^+$ surface species.

At $m_{\text{Si}} = 10^{-3}$ mol/kg, which lies below the solubility of amorphous silica, a change in the spectra accompanied by a significant peak shift is observed. This supports the above mentioned hypothesis that with increasing silicate concentration in solution additional inner-sphere surface species involving silicate can be formed. A possible stoichiometry for the species at $\text{pH}_m = 9$ could be $>\text{SOCm}(\text{OH})_x(\text{SiO}_4)_y(\text{H}_2\text{O})_{4-x}$ (with $x, y = 1, 2$).

Based on this result, the 610 nm species in the illite sorption study might be assigned to a clay/curium/silicate/hydroxo surface complex as the measured aqueous silica concentration is $m_{\text{Si}} = 7 \times 10^{-3}$ mol/kg at $\text{pH}_m > 11$ (Bradbury and Baeyens, 2009).

The increased lifetime of $\tau \sim 165 \pm 15 \mu\text{s}$ at higher pH values supports the hypothesis of a silicate containing Cm surface complex. Similar lifetime values have been reported by Huittinen et al. (2012). The lifetime would be compatible with a $>\text{SOCm}(\text{OH})_x(\text{SiO}_4)_y(\text{H}_2\text{O})_{3-x}$ (with $x, y = 1, 2$) species with silicate binding in a bidentate mode. However, additional studies are required to obtain more information on the exact stoichiometry and structure of this surface complex.

4. SUMMARY AND CONCLUSIONS

Our batch sorption investigations, TRLFS experiments and model calculations have resulted in a number of observations relevant to the adsorption of trivalent actinides and lanthanides on clays in aqueous solutions at high salt concentrations. These observations can be summarized as follows:

1. The pH_m dependent sorption data are affected by salinity: With increasing ionic strength the extent of cation adsorption decreases at low pH_m as expected for ion-exchange. At $\text{pH}_m > 8$ experimentally observed uptake is nearly quantitative even for the very high salt contents. The concentration of dissolved Eu(III) species lies at or below analytical detection limits.
2. The experimental data of the uptake studies can be well predicted for very high salt content using the model developed by Bradbury and Baeyens for low ionic strengths when the appropriate activity corrections are made to the dissolved species and water. Both Pitzer and SIT approach provide very similar results and predict decreasing sorption at $\text{pH}_m > 8$ with increasing ionic strength, which is not observed by experiment. Still, deviations of modelled and experimental Eu(III) uptake curves lie within the uncertainties of experimental data and model parameters at least for $I = 0.09$ and 0.92 molal. A slight variation of less than one log K would significantly improve the fit. We noted that ternary interaction parameters are missing in the aqueous solution speciation data base of the Pitzer framework for trivalent actinides/lanthanides in the NaCl system, which however has a minor effect for the present study.
3. The spectroscopic studies support the idea that there is no significant change in surface speciation within the large variation in NaCl concentration that was studied. Cm-surface complexes with chloride in the second shell could not be detected. However, a surface species occurs at high pH which appears to be related to the interaction of adsorbed Cm with dissolved silicate.

ACKNOWLEDGMENTS

We are grateful to Maria Marques Fernandes (The Laboratory for Waste Management (LES) Paul-Scherrer-Institute Switzerland) for providing the purified Illite du Puy and Na-SWy-2. The research has received partially funding from the German Federal Ministry for Economic Affairs and Energy (BMWi) under contract no. 02 E 10961. The constructive reviews by three anonymous referees are highly appreciated.

APPENDIX A. SUPPLEMENTARY INFO

Supplementary info from this article can be found in the online version.

REFERENCES

- Altmaier M., Metz V., Neck V., Müller R. and Fanghänel Th. (2003) Solid-liquid equilibria of $\text{Mg}(\text{OH})_2(\text{cr})$ and $\text{Mg}_2(\text{OH})_3\text{Cl}\cdot 4\text{H}_2\text{O}(\text{cr})$ in the system Mg-Na-H-OH-Cl- H_2O at 25°C. *Geochim. Cosmochim. Acta* **67**, 3595-3601.
- Ams D. A., Swanson J. S., Szymanowski J. E. S., Fein J. B., Richmann M. and Reed D. T. (2013) The effect of high ionic strength on neptunium (V) adsorption to a halophilic bacterium. *Geochim. Cosmochim. Acta* **110**, 45-57.
- Andra (2001) Référentiel géologique du site de Meusel Haute Marne. Rapp. A RP ADS 99-005 de l'Agence nationale pour la gestion des déchets radioactifs. Châtenay-Malabry, France.

- Baeyens B. and Bradbury M. H. (2004) Cation exchange capacity measurements on illite using the sodium and cesium isotope dilution technique: effects of the index cation, electrolyte concentration and competition: modeling. *Clay. Clay. Miner.* **52**, 421-431.
- Bethke C. M. and S. Yeakel (2011) The Geochemist's Workbench User's Guides, Version 9.0. Aqueous Solutions LLC, Champaign.
- Bonin B. (1998) Deep geological disposal in argillaceous formations: studies at the Tournemire site. *J. Contam. Hydrol.* **35**, 315-330.
- Bradbury M. H. and Baeyens B. (1997) A mechanistic description of Ni and Zn sorption on Na-montmorillonite Part II: modeling. *J. Contam. Hydrol.* **27**, 223-248.
- Bradbury M. H. and Baeyens B. (2002) Sorption of Eu on Na- and Ca-montmorillonites: Experimental investigations and modeling with cation exchange and surface complexation. *Geochim. Cosmochim. Acta* **66**, 2325-2334.
- Bradbury M. H., Baeyens B., Geckeis H. and Rabung Th. (2005) Sorption of Eu(III)/Cm(III) on Ca-montmorillonite and Na-illite. Part 2: Surface complexation modeling. *Geochim. Cosmochim. Acta* **69**, 5403-5412.
- Bradbury M. H. and Baeyens B. (2006) Modeling sorption data for the actinides Am(III), Np(V) and Pa(V) on montmorillonite. *Radiochim. Acta* **94**, 619-625.
- Bradbury M. H. and Baeyens B. (2009) Sorption modeling on illite. Part I: Titration measurements and the sorption of Ni, Co, Eu and Sn. *Geochim. Cosmochim. Acta* **73**, 990-1003.
- Bradbury M. H. and Fernandes M. M. (2013) Personal communication.

- Brewitz W. (1980) Zusammenfassender Zwischenbericht, GSF T 114.
- Fanghänel Th., Kim J. I., Klenze R. and Kato Y. (1995) Formation of Cm(III) chloride complexes in CaCl₂ solutions. *J. Alloy. Compd.* **225**, 308-311.
- Fritz P. and Frapé S. K. (1982) Saline Groundwaters in the Canadian shield – a first overview. *Chem. Geol.* **36**, 179-190.
- Gaines Jr. G. L. and Thomas H. C. (1953) Adsorption studies on clay minerals. II. A formulation of the thermodynamics of exchange adsorption. *J. Chem. Phys.* **21**, 714-718.
- Geckeis H. and Rabung Th. (2008) Actinide geochemistry: From the molecular level to the real system. *J. Contam. Hydrol.* **102**, 187-195.
- Geckeis H., Lützenkirchen J., Polly R., Rabung Th. and Schmidt M. (2013) Mineral-Water Interface Reactions of Actinides. *Chem. Rev.* **113**, 1016-1062.
- Gorgeon L. (1994) Contribution à la modélisation physico-chimique de la rétention de radioéléments à vie longue par des matériaux argileux, Thèse de doctorat, Université Paris, Paris, France.
- Gustafsson J. P. and Lumsdon D. G. (2014) Comment on “Citrate adsorption can decrease soluble phosphate concentration in soils: Result of theoretical modelling” by Marek Duputel, Nicolas Devau, Michel Brossard, Benoît Jaillard, Davey L. Jones, Philippe Hinsinger and Frédéric Gérard (2013). *Appl. Geochem.* **46**, 85-89.
- Harvie C. E., Møller N. and Weare J. H. (1984) The prediction of mineral solubilities in natural waters: The Na-K-Mg-Ca-H-Cl-SO₄-OH-HCO₃-CO₃-CO₂-H₂O system to high ionic strengths at 25°C. *Geochim. Cosmochim. Acta* **48**, 723-751.

- Huittinen N., Rabung Th., Schnurr A., Hakanen M., Lehto J. and Geckeis H. (2012) New insight into Cm(III) interaction with kaolinite – Influence of mineral dissolution. *Geochim. Cosmochim. Acta* **99**, 100-109.
- Keizer M. G. and van Riemsdijk W. H. (1999) Wageningen University, 6700 HB Wageningen, Holland.
- Nagra (2002) Project opalinus clay: safety report. Demonstration of disposal feasibility (Entsorgungsnachweis) for spent fuel, vitrified high-level waste and long-lived intermediate-level waste. Nagra Technical Report NTB 02-05, Nagra, Wettingen, Switzerland.
- NEA (2003) Update on the chemical thermodynamics of uranium, neptunium, plutonium, americium and technetium. In *Chemical Thermodynamics* vol. 5 (ed. OECD Nuclear Energy Agency). Elsevier, Amsterdam.
- Neck V., Altmaier M., Rabung Th., Lützenkirchen J. and Fanghänel Th. (2009) Thermodynamics of trivalent actinides and neodymium in NaCl, MgCl₂, and CaCl₂ solutions: Solubility, hydrolysis, and ternary Ca-M(III)-OH complexes. *Pure Appl. Chem.* **81**, 1555-1568.
- OECD/NEA (2008) Radioactive Waste Management Committee: „Collective Statement on Moving Forward to Geological Disposal of Radioactive Waste“, ISBN 978-92-64-99057-9.
- Ondraf (2001) SAFIR 2: safety assessment and feasibility interim report 2. NIROND-2001-06 E. Ondraf, Brussels.

- Parkhurst D. L. and Appelo C. A. J. (1999) User's Guide to PHREEQC (version 2), a computer program for speciation, batch-reaction, one-dimensional transport and inverse geochemical calculations. US Geological Survey Water-Resources Investigations Report 99-4259.
- Poinssot C., Baeyens B. and Bradbury M. H. (1999) Experimental and modeling studies of caesium sorption on illite. *Geochim. Cosmochim. Acta* **63**, 3217-3227.
- Rabung Th., Pierret M. C., Bauer A., Geckeis H., Bradbury M. H. and Baeyens B. (2005) Sorption of Eu(III)/Cm(III) on Ca-montmorillonite and Na-illite. Part 1: Batch sorption and time-resolved laser fluorescence spectroscopy experiments. *Geochim. Cosmochim. Acta* **69**, 5393-5402.
- Stumpf S., Stumpf T., Lützenkirchen J., Walther C. and Fanghänel T. (2008) Immobilization of trivalent actinides by sorption onto quartz and incorporation into siliceous bulk: Investigations by TRLFS. *J. Colloid Interf. Sci.* **318**, 5-14.
- Stumpf T., Bauer A., Coppin F. and Kim J. I. (2001) Time-Resolved Laser Fluorescence Spectroscopy Study of the Sorption of Cm(III) onto Smectite and Kaolinite. *Environ. Sci. Technol.* **35**, 3691-3694.
- Stumpf T., Bauer A., Coppin F., Fanghänel T. and Kim J. I. (2002) Inner-sphere, outer-sphere and ternary surface complexes: a TRLFS study of the sorption process of Eu(III) onto smectite and kaolinite. *Radiochim. Acta* **90**, 345-349.
- Tan X., Fang M. and Wang X. (2010) Sorption Speciation of Lanthanides/Actinides on Minerals by TRLFS, EXAFS and DFT Studies: A Review. *Molecules* **15**, 8431-8468.

Tombácz E., Nyilas T., Libor Z. and Csanaki C. (2004) Surface charge heterogeneity and aggregation of clay lamellae in aqueous suspensions. *Prog. Coll. Pol. Sci. S.* **125**, 206-215.

Vilks P. (2011) Sorption of Selected Radionuclides on Sedimentary Rocks in Saline Conditions – Literature Review. NWMO TR-2011-12, Atomic Energy of Canada Limited, Toronto, Ontario, Canada.

ACCEPTED MANUSCRIPT

Table and Figure Captions

Table 1. Constants for hydrolysis and chloride complexation used for Eu in the sorption modeling at infinite dilution (NEA, 2003).

Table 2. Cation exchange capacities and surface hydroxyl group densities for SWy-2 and Illite du Puy (Bradbury and Baeyens, 2006 and 2009).

Table 3. Parameters to model Eu(III)-sorption on Illite du Puy and SWy-2 with the 2SPNE SC/CE model at infinite dilution (Bradbury and Baeyens, 2006 and 2009).

Figure 1. Sorption edges for Eu ($m_{\text{Eu,total}} = 2.0 \times 10^{-7}$ mol/kg), S:L 2 g/L, on Na-illite as a function of pH_m and at different NaCl concentrations. Sorption data (symbols) are presented as percentage uptake (a) and logarithm of distribution ratio ($\log K_D$) (b, c, d). Further investigations (details in text/SI) lead to two more data points (b, green stars). C_m ($m_{Cm} = 2.0 \times 10^{-7}$ mol/kg, S:L 0.25 g/L) sorption data obtained from TRLFS studies are added in (c) (only the contribution of inner-sphere sorption is considered, details see text). Curves represent blind predictions using the 2 SPNE SC/CE model and Pitzer equations (a, b, d) or SIT (c). Simulated Eu surface speciation is shown for $m_{\text{NaCl}} = 3.90$ mol/kg in (a). Result for calculations (applying Pitzer equations) with slightly modified surface complexation constants (numbers in brackets in Tab. 3) to better fit our experimental data (see respective discussion in the text) (d).

Figure 2. Sorption edges for Eu ($m_{\text{Eu,total}} = 2.0 \times 10^{-7}$ mol/kg), S:L 2 g/L, on Na-SWy-2 montmorillonite as a function of pH_m and at different NaCl concentrations. Sorption data (symbols) are presented as logarithm of distribution ratio ($\log K_D$). Curves represent blind predictions using the 2 SPNE SC/CE model and Pitzer equations (a). Result for calculations (applying Pitzer equations) with slightly modified surface complexation constants (number in

brackets in Tab. 3) to better fit our experimental data (see respective discussion in the text)

(b).

Figure 3. Na-illite: Cm(III) fluorescence spectra normalized to the same peak area and positions of the peak maxima of the pure component spectra as straight lines; $[Cm] = 2.0 \times 10^{-7}$ mol/kg, S:L ratio = 0.25 g/L, 0.10 mol/kg NaCl solution (chosen pH values, for more details see supplementary information).

Figure 4. (a) Na-illite, (b) Na-SWy-2: Pure component spectra derived from peak deconvolution of measured fluorescence spectra obtained at each ionic strength (0.10, 4.37 mol/kg; 1.02 is shown in the supplementary info).

Figure 5. Cm(III) fluorescence spectra normalized to the same peak height with different amounts of added Si concentrations ($m_{Si} = 10^{-5}, 10^{-4}, 10^{-3}$ mol/kg) in presence of illite at $pH_m = 9$.

Aqueous complexation reactions	log K
$Eu^{3+} + H_2O \rightleftharpoons Eu(OH)^{2+} + H^+$	-7.2
$Eu^{3+} + 2 H_2O \rightleftharpoons Eu(OH)_2^+ + 2 H^+$	-15.1
$Eu^{3+} + 3 H_2O \rightleftharpoons Eu(OH)_3 + 3 H^+$	-26.2
$Eu^{3+} + Cl^- \rightleftharpoons EuCl^{2+}$	0.24
$Eu^{3+} + 2 Cl^- \rightleftharpoons EuCl_2^+$	-0.74

Table 1

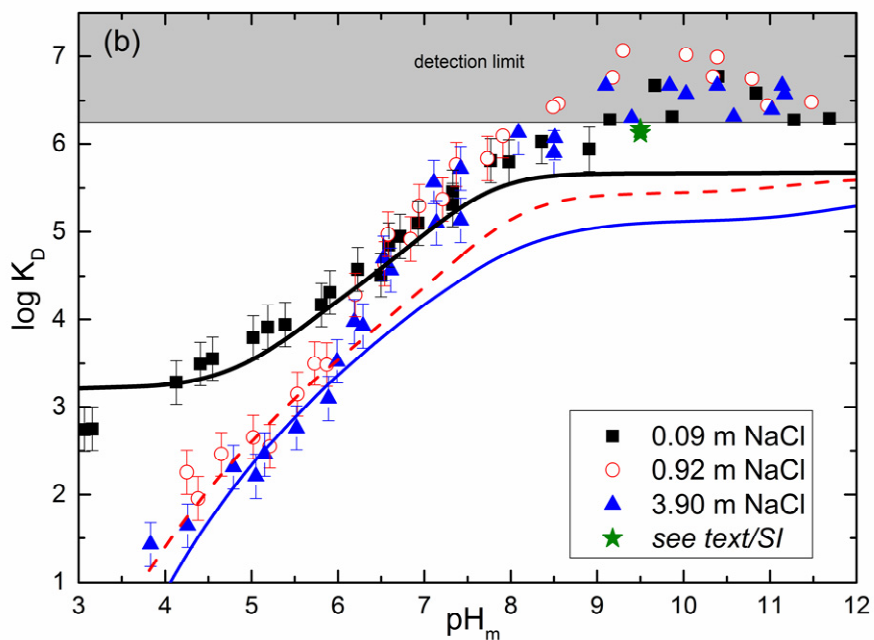
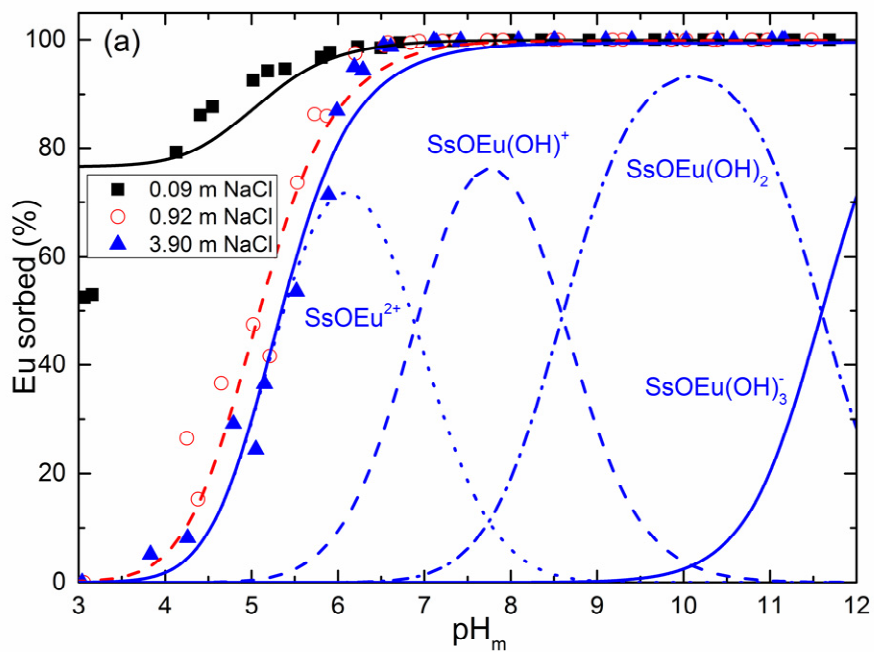
Site types	Na-SWy-2	Na-illite
	Site capacities	Site capacities
S ^S OH	2.0 x 10 ⁻³ mol/kg	2.0 x 10 ⁻³ mol/kg
S ^{W1} OH	4.0 x 10 ⁻² mol/kg	4.0 x 10 ⁻² mol/kg
S ^{W2} OH	4.0 x 10 ⁻² mol/kg	4.0 x 10 ⁻² mol/kg
CEC	8.7 x 10 ⁻¹ eq/kg	2.25 x 10 ⁻¹ eq/kg

Table 2

	Na-SWy-2	Na-illite
Surface protolysis reactions:		
$S^S OH + H^+ \rightleftharpoons S^S OH_2^+$	4.5	4.0
$S^S OH \rightleftharpoons S^S O^- + H^+$	-7.9	-6.2
$S^{W1} OH + H^+ \rightleftharpoons S^{W1} OH_2^+$	4.5	4.0
$S^{W1} OH \rightleftharpoons S^{W1} O^- + H^+$	-7.9	-6.2
$S^{W2} OH + H^+ \rightleftharpoons S^{W2} OH_2^+$	6.0	8.5
$S^{W2} OH \rightleftharpoons S^{W2} O^- + H^+$	-10.5	-10.5
Surface complexation reactions:		
$S^S OH + Eu^{3+} \rightleftharpoons S^S OEu^{2+} + H^+$	2.3*	1.9
$S^S OH + Eu^{3+} + H_2O \rightleftharpoons S^S OEu(OH)^+ + 2 H^+$	-5.9*	-4.6 (-4.1)
$S^S OH + Eu^{3+} + 2 H_2O \rightleftharpoons S^S OEu(OH)_2 + 3 H^+$	-14.2* (-13.9)	-12.8 (-12.0)
$S^S OH + Eu^{3+} + 3 H_2O \rightleftharpoons S^S OEu(OH)_3^- + 4 H^+$	(-25.8)	-24.0 (-23.2)
Cation exchange reactions:		
$3 \text{ Na-clay} + Eu^{3+} \rightleftharpoons \text{Eu-clay} + 3 Na^+$	1.5	1.9

* Am(III) surface complexation reactions are used to simulate Eu(III). Slightly varied surface complexation constants (values in brackets) are taken for scoping calculations in order to provide for a better fit to the experimental data (see discussion in the text)

Table 3



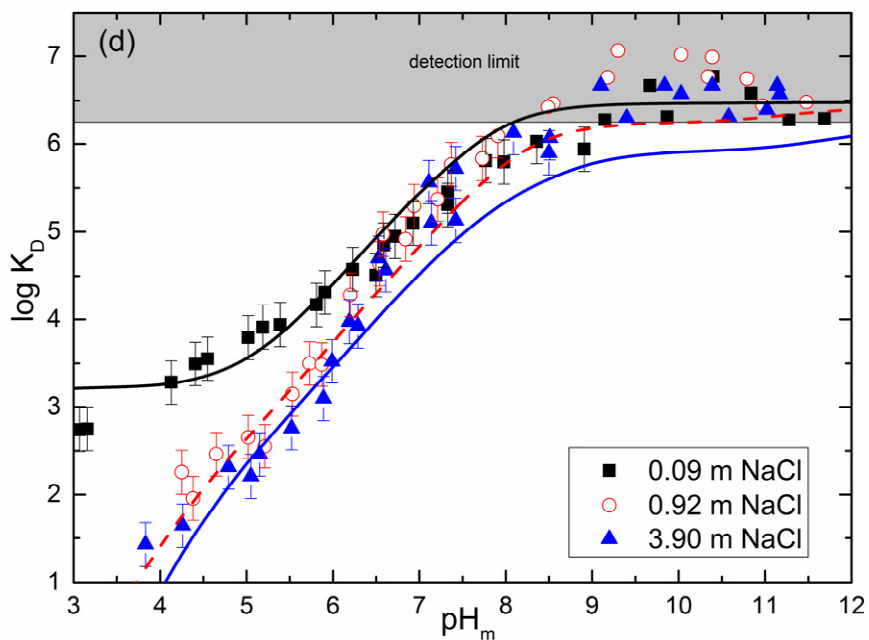
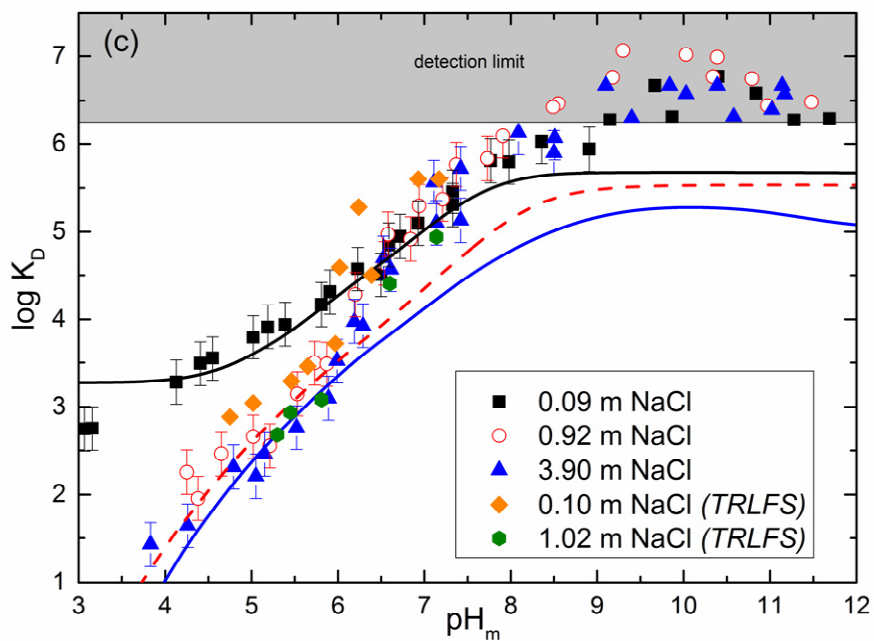


Figure 1

ACCEPTED MANUSCRIPT

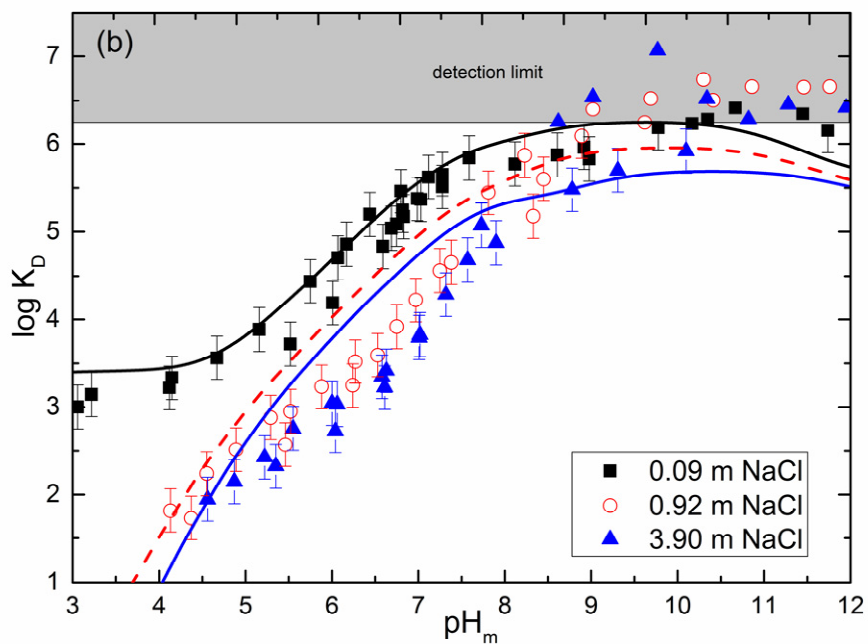
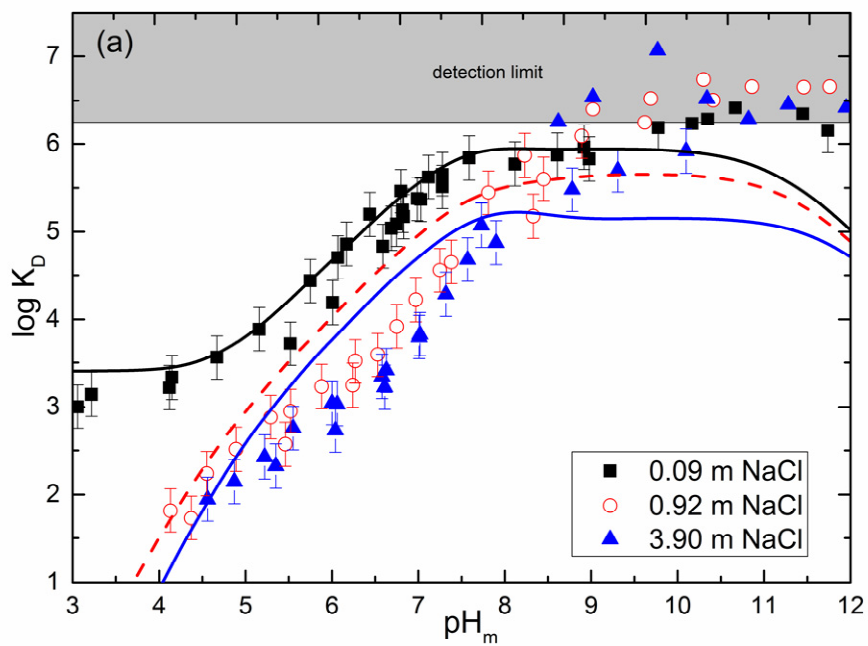


Figure 2

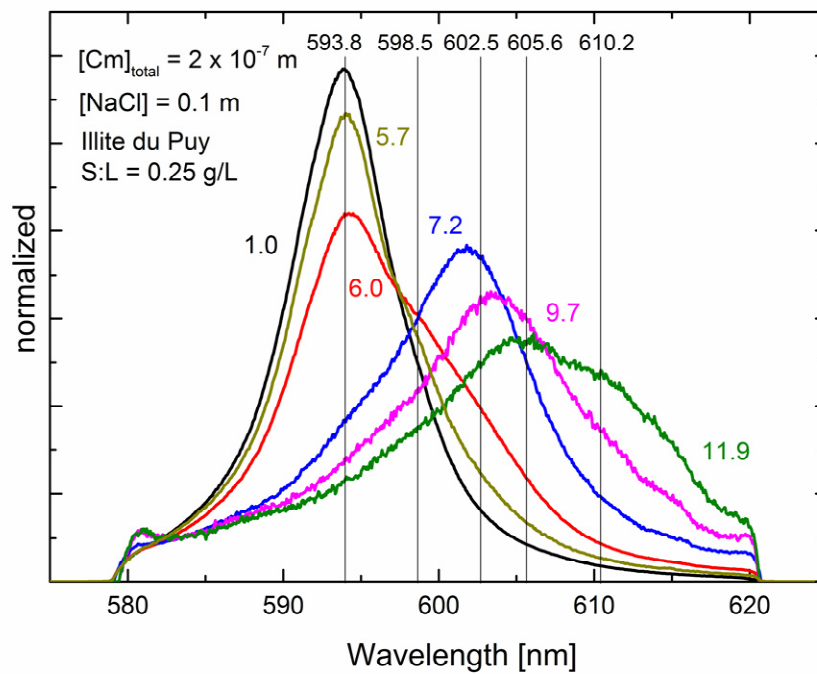


Figure 3

ACCEPTED

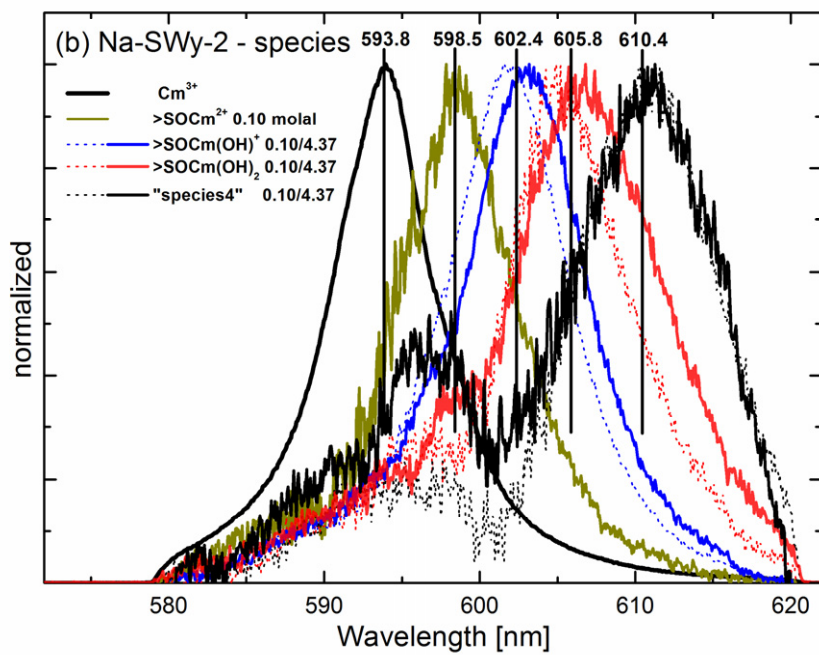
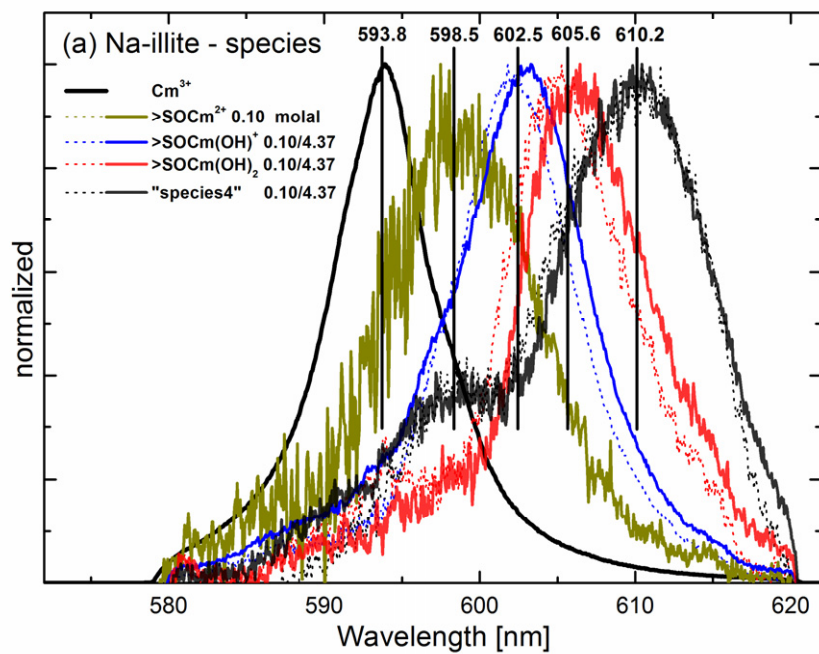


Figure 4

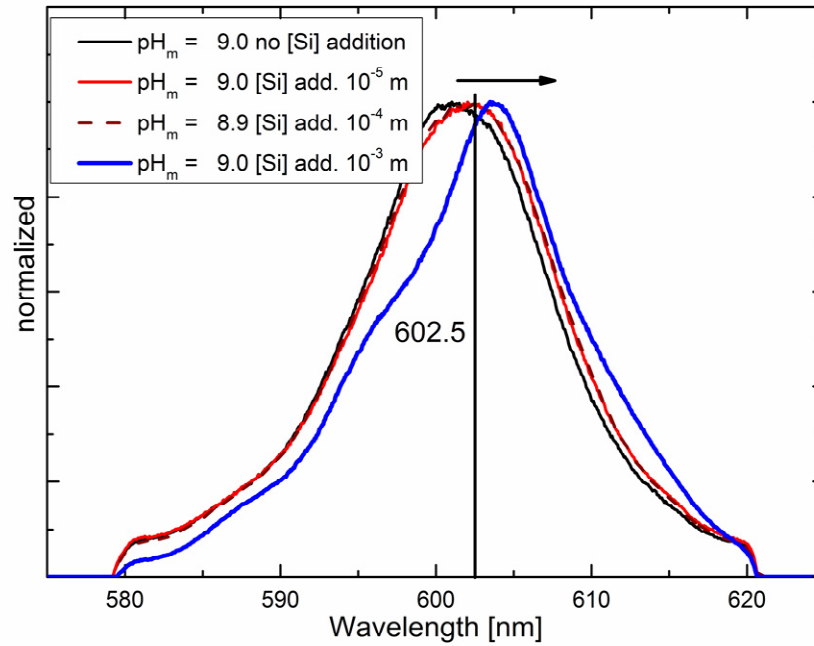


Figure 5

ACCEPTED